

Quintessential inflation in Palatini $F(R, X)$ gravity

Konstantinos Dimopoulos^a Christian Dioguardi^{b,c} Gert Hütsi^c
Antonio Racioppi^c

^aConsortium for Fundamental Physics, Physics Department, Lancaster University, Lancaster
LA1 4YB, United Kingdom

^bTallinn University of Technology, Akadeemia tee 23, 12618 Tallinn, Estonia

^cNational Institute of Chemical Physics and Biophysics, Rävala 10, 10143 Tallinn, Estonia

E-mail: konst.dimopoulos@lancaster.ac.uk, christian.dioguardi@kbfi.ee,
antonio.racioppi@kbfi.ee, gert.hutsi@kbfi.ee

Abstract. Palatini $F(R, X)$ gravity, with X the inflaton kinetic term, proved to be a powerful framework for generating asymptotically flat inflaton potentials. Here we show that a quadratic Palatini $F(R, X)$ restores compatibility with data of the Peebles-Vilenkin quintessential model. Moreover, the same can be achieved with an exponential version of the Peebles-Vilenkin potential if embedded in a Palatini $F(R, X)$ of order higher than two.

Keywords: Quintessence, Inflation, Dark Energy, Palatini gravity

Contents

1	Introduction	1
2	Palatini $F(R, X)$ framework	3
3	Quintessential inflation for $F(R_X) = R_X + \alpha R_X^2$	4
3.1	Inflation	4
3.2	Kination	6
3.3	Reheating	7
3.4	Quintessence	7
3.5	The case of the exponential tail	9
4	Quintessential inflation for $F(R_X)_{>2}$	12
4.1	Exponential PV potential	13
4.2	A note on the exponential tail	15
5	Conclusions	15
A	Constraints from the overproduction of GWs	16

1 Introduction

The Λ CDM model represents today the Standard Cosmological Model. The main ingredients of the model are a relativistic matter component (radiation), some non-relativistic matter (cold dark matter, baryonic matter) and a cosmological constant, Λ , associated with dark energy. The latter drives the current accelerated expansion of the Universe.

Λ CDM, while being a simple model, requires extreme fine tuning. The most popular way of improving Λ CDM is by introducing a scalar field, called quintessence in the literature (e.g. [1, 2] and refs. therein), that in contrast to Λ is a dynamical field. If the field varies slowly and has the appropriate energy density today then it can lead to the aforementioned accelerated expansion at present.

At the same time, observations of the cosmic microwave background radiation (CMB) support the idea of a spatially flat and isotropic Universe at large scales, which can be explained by assuming cosmic inflation, i.e. another accelerated expansion of the Universe but during its very early stages [3–6]. In its simplest realization the inflation is driven by another scalar field, the inflaton, with an almost flat potential energy.

Although similar in principle, inflation and dark energy late-time acceleration happen at very different energy scale, respectively around 10^{16} GeV and 10^{-12} GeV. Hence, the two phenomena are usually considered to have different origin. At the same time having an extra quintessence field introduces the coincidence problem: one has to require specific initial conditions so that the currently energy density of the scalar field matches the observed value of the cosmological constant.

Building a model of quintessential inflation overcomes this issue, by realizing the initial condition for quintessence through inflation [7]. However, a working model of the quintessential inflation must satisfy several conditions. First of all it has to provide a graceful exit from

inflation, providing good predictions for the CMB observables. Second, the scalar field has to survive until present days, this implies that a reheating mechanism that does not rely on its decay has to be provided such as instant preheating [8, 9], curvaton reheating [10, 11], gravitational reheating [12–14], Ricci reheating [15–17], reheating by primordial black hole evaporation [18, 19], warm quintessential inflation [20, 21], to name but some. Finally, the scalar field potential needs to be very steep in order to bridge the energy gap between inflation and quintessence, allowing for a period of kination, which eventually ends due to reheating. This will eventually lead to the freezing of the scalar field at a value such that its energy density matches the value corresponding to the observed dark energy density.

Several models of quintessential inflation have been built by embedding a scalar field in General Relativity (e.g. [7, 22–25] and references therein). On the other hand, Palatini modifications of Einstein gravity proved to be very powerful tools in quintessential inflation model building (e.g. [26–30] and the references therein). In the standard metric formulation, the only dynamical degree of freedom is the metric tensor, while the affine connection is assumed a priori to be the Levi-Civita one. In the Palatini formulation instead, both the metric and the connection are considered independent dynamical degrees of freedom, and their relation is set by their corresponding equations of motion (EoM). If the action is given by the simple Einstein-Hilbert term, the two formulations are equivalent while in non-minimal theories of gravity they lead to substantially different phenomenological predictions, e.g. [31, 32].

In this article, we are interested in a particular class of non-minimal Palatini models: the $F(R, X)$ models, with X the inflaton kinetic term. Inflation in this class of theories has been extensively studied in [33–35] as an extended generalization of the $F(R)$ models already explored in [34, 36]. The $F(R, X)$ models allow to simplify the structure of the scalar field kinetic term in the Einstein frame and consequently heal the dynamical issues of the $F(R)_{>2}$ (that is those containing terms diverging faster than R^2) theories out of the slow-roll regime. Remarkably, the $F(R, X)_{>2}$ theories, once the consistency criteria are satisfied, universally provide potential apparently suitable for quintessential inflation [33, 34].

The purpose of this work is to find, within the Palatini $F(R, X)$ framework, quintessential inflation setups that describe both inflation in the early Universe and the current accelerated expansion in agreement with the current observational data. The paper is organized as follows. In section 2 we introduce the formalism of Palatini $F(R, X)$ theories. In section 3 we consider the quadratic choice and compute the observables of the model for the Peebles-Vilenkin (PV) potential [7], for inflation, reheating and dark energy, showing the parameter space for which quintessential inflation is viable. At the end of the same section we briefly consider an exponential tail and prove that, while giving very good predictions for the inflation CMB observables, it cannot predict a good quintessential tail for dark energy. In section 4 we consider a specific $F(R, X)_{>2}$ model and compute the results for an exponential version of the PV potential. Finally in section 5 we summarize the results of the paper and draw the conclusions.

We use geometric units where $c = \hbar = k_B = 1$ and $8\pi G = m_P^{-2} = 1$, while the signature of the metric is spacelike.

2 Palatini $F(R, X)$ framework

The starting point for the Palatini $F(R, X)$ models is the following action:

$$S = \int d^4x \sqrt{-g^J} \left(\frac{1}{2} F(R_X) - V(\phi) \right), \quad (2.1)$$

with F is an arbitrary function of its argument, $R_X = R + X$ where $X = -g^{\mu\nu} \partial_\mu \phi \partial_\nu \phi$ is the scalar field kinetic term and $R = g^{\mu\nu} R_{\mu\nu}(\Gamma)$ is the Palatini Ricci scalar built from the metric-independent Ricci tensor, with Γ denoting the connection. We can rewrite the action (2.1) by introducing an auxiliary field ζ as follows:

$$S = \int d^4x \sqrt{-g^J} \left(\frac{1}{2} F(\zeta) + \frac{1}{2} F'(\zeta) (R - g^{\mu\nu} \partial_\mu \phi \partial_\nu \phi - \zeta) - V(\phi) \right). \quad (2.2)$$

By means of a conformal transformation $g_{\mu\nu}^E = F'(\zeta) g_{\mu\nu}^J$, we can rewrite the action in the Einstein frame, where the theory is linear in R and minimally coupled to the metric $g_{\mu\nu}^E$:

$$S = \int d^4x \sqrt{-g^E} \left(\frac{R}{2} - \frac{1}{2} g_E^{\mu\nu} \partial_\mu \phi \partial_\nu \phi - U(\zeta, \phi) \right), \quad (2.3)$$

with

$$U(\zeta, \phi) = \frac{V(\phi)}{F'(\zeta)^2} - \frac{F(\zeta)}{2F'(\zeta)^2} + \frac{\zeta}{2F'(\zeta)}. \quad (2.4)$$

By taking the variation with respect to ζ we get the corresponding equation of motion:

$$G(\zeta) = \frac{1}{4} (2F(\zeta) - \zeta F'(\zeta)) = V(\phi), \quad (2.5)$$

which can be solved to get $\zeta(\phi)$. Equation (2.5) was already introduced in [36] where it holds as an approximation valid in the slow-roll regime. However, in this case, eq. (2.5) is exact and valid even in the presence of large kinetic terms for the canonical scalar field. In other words, the auxiliary field $\zeta = \zeta(\phi)$ is a function of the canonically normalized field only and not of its derivatives. By using eq. (2.5) one can rewrite $U(\zeta, \phi)$ in eq. (2.4) in terms of ζ only, obtaining

$$U(\zeta) = \frac{\zeta}{4F'(\zeta)}. \quad (2.6)$$

This implies that even in the cases for which $G(\zeta)$ cannot be explicitly solved in terms of ζ , it can still be exploited for computing the inflationary observables [36]. In all the other (few) cases, $\zeta = \zeta(\phi)$ can be explicitly determined, allowing computations to proceed in the standard way.

In the following, we study two types of $F(\zeta)$ functions. First we consider a quadratic $F(\zeta)$ which has the property to automatically flatten any diverging $V(\phi)$ when $\zeta \rightarrow +\infty$ (see eqs. (2.5) and (2.6)). Then, we study a $F(\zeta)_{>2}$ i.e. a $F(\zeta)$ of order higher than two. This is a very special case because, first of all, in order to have a viable solution of eq. (2.5), $V(\phi)$ must be negative [33, 34]. Secondly, even though $V(\phi) < 0$, the Einstein frame potential $U(\zeta)$ in eq. (2.6) is positive as long as $\zeta, F'(\zeta) > 0$. Finally, since $F(\zeta)$ is of order higher than two, $F'(\zeta)$ is of order higher than one, implying that at $\zeta \rightarrow +\infty$, $U(\zeta)$ automatically develops a tail approaching zero, which is exactly one of the requirements for quintessence.

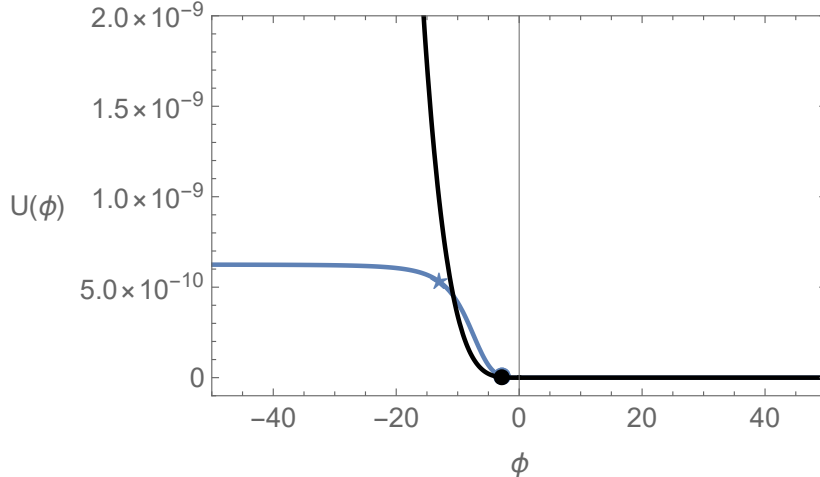


Figure 1: The PV potential (black), and the modified PV potential (blue) with $\alpha = 2 \cdot 10^8$, $q = k = 4$, predicting viable CMB observables $r = 0.017$, $n_s = 0.966$ (at $N_e = 60$) and a quintessential tail the solves the coincidence problem at the mass scale $M = 1.38 \cdot 10^{-13}$. We also show ϕ_N (star) and ϕ_{end} (dot) in the same color code. ϕ_N is not visible for the original PV potential as it lays at $V(\phi_N) \sim 10^{-8}$. We notice that while the potential is modified at the inflation scale, it remains unchanged in the tail.

3 Quintessential inflation for $F(R_X) = R_X + \alpha R_X^2$

This setup has been introduced in the context of fractional attractors in [33]. In such a scenario, $G(\zeta) = \frac{1}{4}\zeta = V(\phi)$ which implies that the Einstein frame potential takes the simple form

$$U(\phi) = \frac{V(\phi)}{1 + 8\alpha V(\phi)}, \quad (3.1)$$

where we can immediately see that $U \rightarrow 0(\frac{1}{8\alpha})$ when $V \rightarrow 0(+\infty)$. Therefore, in order to have a quintessential tail for the potential we need to consider a form of $V(\phi)$ with a decreasing tail. The simplest example is the PV potential, the first model made to describe quintessential inflation [7]. The Jordan frame potential has then following form:

$$V(\phi) = \begin{cases} \lambda^k(\phi^k + M^k) & \phi \leq 0 \\ \lambda^k \frac{M^{k+q}}{\phi^q + M^q} & \phi > 0, \end{cases} \quad (3.2)$$

with k an even number. We stress that such a configuration shares a similar form for the Einstein frame scalar potential as in ref. [26]. However, in ref. [26] the scalar field also needs to undergo a canonical normalization, while in our set-up ϕ is already canonical normalized. This implies different phenomenological results with respect to ref. [26].

3.1 Inflation

The original PV potential does not satisfy the experimental bounds from the CMB observations [37]. In our case instead, by starting from a Jordan frame potential with the form of the PV potential we obtain an Einstein frame potential with a plateau in the inflationary region, as shown in Fig. 1.

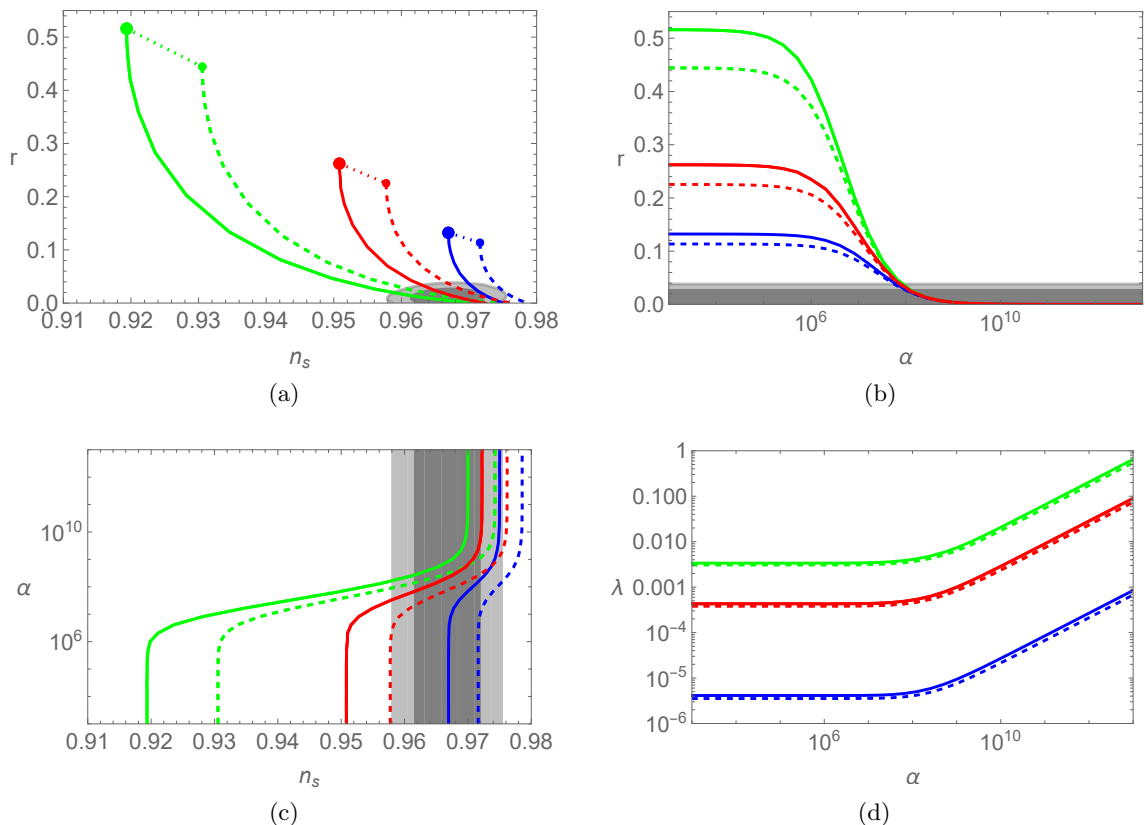


Figure 2: r vs. n_s (a), r vs. α (b), α vs. n_s (c), λ vs. α (d) for the PV potential with $k = 2$ (blue), $k = 4$ (red), $k = 8$ (green) for $N_e = 60$ (thick) and $N_e = 70$ (dashed). The dots represents the predictions of the of the original PV potential in the same color code. The gray regions indicate the 95% (dark-gray) and 68% (light-gray) confidence levels (CL), respectively, based on the latest combination of Planck, BICEP/Keck, and BAO data [37].

We plot the original PV potential (black), and the modified PV potential in eq. (3.1) (blue) with $\alpha = 2 \cdot 10^8$, $q = k = 4$, predicting viable CMB observables $r = 0.017$, $n_s = 0.966$ (at $N_e = 60$) and a quintessential tail that solves the coincidence problem with the mass scale $M = 1.38 \cdot 10^{-13}$. We also show ϕ_N (star) and ϕ_{end} (dot) in the same color code. ϕ_N is not visible for the original PV potential as it lies at $V(\phi_N) \sim 10^{-8}$. We notice that, while the potential is modified at the inflation scale, it remains unchanged in the tail. This is indeed expected. By taking the limit $\phi \rightarrow -\infty$ of eqs. (3.1) and (3.2), we see that $U(\phi) \rightarrow \frac{1}{8\alpha}$ which sets the height of the inflationary plateau. On the other hand, for $\phi \rightarrow \infty$ we get $U(\phi) \sim V(\phi)$, which reproduces the behavior of the original potential.

We now study the details of the inflationary phenomenology. The slow-roll parameters read

$$\epsilon(\phi_N) = \frac{k^2 \phi_N^{2k-2}}{2 (M^k + \phi_N^k)^2 (8\alpha \lambda^k \phi_N^k + 8\alpha \lambda^k M^k + 1)^2}, \quad (3.3)$$

$$\eta(\phi_N) = \frac{k \phi_N^{k-2} (-8\alpha k \lambda^k \phi_N^k - 8\alpha \lambda^k \phi_N^k + 8\alpha k \lambda^k M^k - 8\alpha \lambda^k M^k + k - 1)}{(M^k + \phi_N^k) (8\alpha \lambda^k \phi_N^k + 8\alpha \lambda^k M^k + 1)^2}, \quad (3.4)$$

and the number of e -folds is:

$$N_e = \left[\frac{\phi^{2-k}}{2k} \left(\frac{\phi^k (16\alpha\lambda^k\phi^k + k + 2)}{k + 2} - \frac{16\alpha\lambda^k M^{2k}}{k - 2} + 2M^k \left(8\alpha\lambda^k\phi^k + \frac{1}{2 - k} \right) \right) \right]_{\phi_{end}}^{\phi_N}. \quad (3.5)$$

In the strong coupling limit for $\alpha \rightarrow \infty$, $\phi_N \rightarrow -\infty$, and neglecting the contribution of ϕ_{end} the inflationary observables can be approximated as:

$$N_e \simeq \frac{8\alpha\lambda^k\phi_N^{k+2}}{k(k+2)}, \quad (3.6)$$

$$r \simeq \frac{1}{12\pi^2\alpha A_s}, \quad (3.7)$$

$$n_s \simeq 1 - \frac{k+1}{k+2} \frac{2}{N_e}, \quad (3.8)$$

$$A_s \simeq \frac{k+2}{12\pi^2 k} \lambda^k N_e \left(\frac{k(k+2)N_e}{8\alpha\lambda^k} \right)^{\frac{k}{k+2}}. \quad (3.9)$$

We plot in Fig. 2 the numerical results for slow-roll inflation using this model. Notice that the number of e -folds is chosen in the range $N_e = 60 - 70$ instead of the usual $N_e = 50 - 60$, due to kination contribution during the Universe expansion, which is absent in models that consider anoscillatory reheating mechanism. The relation between λ, α is imposed by fixing $A_s = 2.1 \cdot 10^{-9}$ [38]. From Fig. 2 we can see that agreement with data can easily be achieved with $\alpha \gtrsim 10^8$. To conclude, we note that the asymptotic results given in eqs. (3.7) and (3.8) are exactly the same as the ones obtained in [33] because in the inflationary region the models are equivalent in the big α region.

3.2 Kination

Right after the end of inflation the equation of motion for the Einstein frame scalar field:

$$\ddot{\phi} + 3H\dot{\phi} + V'(\phi) = 0, \quad (3.10)$$

becomes dominated by kinetic energy and can be approximated as:

$$\ddot{\phi} + 3H\dot{\phi} \simeq 0. \quad (3.11)$$

The solution for $\dot{\phi}$ is given by

$$\dot{\phi} = \sqrt{\frac{2}{3}} \frac{1}{t}. \quad (3.12)$$

Hence, by assuming that the scalar field behaves as a perfect fluid we have:

$$\rho_\phi = \frac{1}{2}\dot{\phi}^2 + V(\phi) \sim \frac{1}{2}\dot{\phi}^2 \propto a^{-6}, \quad (3.13)$$

with $a \propto t^{1/3}$. Since from the Friedmann equations we have that $\rho \propto a^{-3(1+w)}$, during kination the scalar field behaves as a barotropic fluid with $w = 1$. By direct integration we have from eq. (3.12):

$$\phi(t) = \phi_{end} + \sqrt{\frac{2}{3}} \ln \left(\frac{t}{t_{end}} \right). \quad (3.14)$$

Kination finally needs to end in order to let the Hot Big Bang (HBB) take place. This has to happen before Big Bang Nucleosynthesis (BBN), so to reproduce the correct abundances of primordial nuclei. Since radiation scales as $\rho_r \propto a^{-4}$, as the Universe expands radiation will eventually become the dominant source of the energy-matter content of the Universe. This process is called reheating, and it can happen right after inflation ends or later on depending on the energy density of radiation at the end of inflation. The main constraint is that transition from kination to radiation domination has to happen before BBN takes place.

3.3 Reheating

We consider that radiation first appears at the end of inflation. We define:

$$\Omega_r^{grav}|_{end} \equiv \frac{\rho_r^{grav}}{\rho}|_{end} \quad (3.15)$$

the density parameter for radiation at the end of inflation. Its specific value will depend on the choice of the reheating mechanism, and in particular the following general condition holds:

$$\Omega_r^{grav}|_{end} \leq \Omega_r|_{end} \leq 1, \quad (3.16)$$

where the upper bound is found by choosing prompt reheating, while the lower bound is set by gravitational reheating which is the weakest reheating mechanism and hence produces the lowest possible value for the density parameter of radiation. The HBB starts with reheating and takes place at time given by:

$$t_{reh} = \frac{t_{end}}{(\Omega_r|_{end})^{3/2}}, \quad (3.17)$$

which implies:

$$\phi_{reh} = \phi_{end} - \sqrt{\frac{3}{2}} \ln(\Omega_r|_{end}). \quad (3.18)$$

Note that ϕ_{reh} only depends on the potential $U(\phi)$ implicitly through the end of inflation, but its derivation is model-independent. Now if we assume that radiation has the time to thermalize by the beginning of radiation domination then we can compute the reheating temperature as:

$$T_{reh} = \left(\frac{30}{\pi^2 g_*^{reh}} (\Omega_r^{end})^3 \rho_\phi^{end} \right)^{1/4}, \quad (3.19)$$

where g_*^{reh} are the effective relativistic degrees of freedom at the time of reheating. In the following we keep Ω_r^{end} as a free parameter, i.e. we do not assume any specific reheating mechanism and proceed to constraint the reheating temperature a posteriori.

3.4 Quintessence

During radiation domination as the Universe keeps expanding; the field loses its kinetic energy while rolling down the field until it freezes. Since the potential is still negligible the EoM for the scalar field is still given by eq. (3.11), but H is now determined by the radiation content of the Universe so the equation yields:

$$\dot{\phi} = \sqrt{\frac{2}{3}} \frac{t_{reh}}{t^3}. \quad (3.20)$$

Hence, by integrating it we get:

$$\phi(t) = \phi_{reh} + 2\sqrt{\frac{2}{3}}\left(1 - \frac{t_{reh}}{t}\right). \quad (3.21)$$

By using eqs. (3.18) and (3.21), we get that the scalar field freezes at $t \gg t_{reh}$ at the value:

$$\phi_F = \phi_{end} + \sqrt{\frac{2}{3}}\left(2 - \frac{3}{2} \ln \Omega_r^{end}\right). \quad (3.22)$$

In order to have a working quintessential inflation mechanism, we need to satisfy two more requirements. The first one is that the value of the scalar field potential energy-density at freezing must match the value of the observed energy density of dark energy today (coincidence requirement), that is:

$$U(\phi_F) = \lambda^k \frac{M^{k+q}}{\phi_F^q + M^q} = \rho_0 \sim 7 \cdot 10^{-121}. \quad (3.23)$$

Second, we need to check that the barotropic parameter at present w_0 for the quintessential tail is within the Planck observational bounds [39]. In order for this to happen we need to make sure that the scalar field unfreezes only at the time of matter-dark energy equality. In other words, the field stays frozen until recent times and only unfreezes when it becomes dominating.

It is a well-known fact that in quintessence models, a competitor attractor behavior can appear. This attractor behavior is referred to in the literature as a tracker, if it leads to eventual quintessence domination. The condition for the tracker to appear is given by:

$$\Gamma \equiv \frac{UU''}{(U')^2} > 1. \quad (3.24)$$

Note that, for an inverse-power-law potential like the one we have chosen, the tracker condition gives $\Gamma = \frac{q+1}{q}$ which implies that the tracker is always present. For the case $q = 4$ the tracker solution for the energy density is $\rho_T \sim (\lambda^4 M^8 / t^4)^{1/3}$, which scales slower than a matter-dominated background.

While the field is frozen at ϕ_F it has a constant contribution to the energy-density. However, if it hits the tracker before becoming dominant it unfreezes and starts following the tracker solution. Eventually, the scalar field becomes dominant with a barotropic parameter $w = -\frac{1}{3}$, which is not acceptable given the observational bound $w_{DE} < -0.95$ [39]. If, on the other hand, the value of $U(\phi_F)$ is small enough i.e. $U(\phi_F(t_{eq})) < \rho_T(t_{eq})$, then the scalar field unfreezes only at the matter-dark energy equality. This imposes a lower bound on the mass scale $M = M_{min}$ in our potential (see Table 1). After dominating, the field thaws and starts slow-rolling down its potential. The slow-rolling quintessence evolves as a fluid with a barotropic parameter given by:

$$w_\phi = \frac{\frac{1}{2}\dot{\phi}^2 - U(\phi)}{\frac{1}{2}\dot{\phi}^2 + U(\phi)} \sim -1, \quad (3.25)$$

since the field changes very slowly with time. It can be checked numerically that field does not evolve substantially from matter-dark energy equality to the present day. Therefore, it is

α	$M_{min}[GeV]$	ϕ_F^{min}	$T_{reh}^{max}[GeV]$	$T_{reh}^*[GeV]$
10^8	$2.0 \cdot 10^5$	4.01	$4.6 \cdot 10^2$	$1.3 \cdot 10^7$
10^{10}	$8.7 \cdot 10^4$	4.01	$4.9 \cdot 10^4$	$3.1 \cdot 10^6$
10^{12}	$2.7 \cdot 10^4$	4.01	$2.3 \cdot 10^3$	$1.9 \cdot 10^5$
10^{14}	$8.7 \cdot 10^3$	4.01	26.3	$1.0 \cdot 10^4$
10^{16}	$2.7 \cdot 10^3$	4.01	0.27	$5.9 \cdot 10^2$

Table 1: Results for reheating for the PV potential (3.2) with $q = k = 4$. The estimated maximum reheating temperature for the model T_{reh}^{max} is below the lower bound T_{reh}^* for every choice of α , this implies that in general the model cannot account for the BBN constraints on overproduction of GWs (see appendix A). However compatibility with observations is restored if one assumes production of heavy particles in the early universe [14].

safe to consider $\phi_0 \simeq \phi_F$ and $w_\phi \approx -1$. We show in Table 1 the results for the case $k = q = 4$. We only report the values of α that allow good predictions for the CMB observables. The value M_{min} is the minimum value of the mass scale for the potential in eq. (3.2) necessary to avoid the tracker solution and let the field unfreeze only at matter-dark energy equality. The corresponding ϕ_F^{min} is obtained by imposing the solution of the coincidence problem in eq. (3.23). The reheating temperature is computed by means of eq. (3.19) by setting $M = M_{min}$ and $\phi = \phi_{min}$.

Finally, we need to check if the model can satisfy the constraints on T_{reh} coming from gravitational-wave (GW) overproduction. During kination, the $w = 1$ stiff period induces a spike in the density of the GWs, potentially spoiling BBN. This can be avoided if T_{reh} is large enough. The details on the calculation can be found in appendix A, while we show in Table 1 an estimate of the lower bound T_{reh}^* (depending on the value of α) that avoids GW overproduction.

Unfortunately, we always have $T_{reh}^{max} < T_{reh}^*$ hence the model is not viable in general. However, compatibility with observation can be restored if we assume the gravitational production of very massive particles after the inflationary era [14]. How much the bound on reheating temperature relaxes, depends on the exact properties of such heavy particles, like mass, heating efficiency etc. However, regardless of the aforementioned details, an indicative validity range can be estimated to be [14]

$$1 \text{ MeV} \leq T_{reh} \leq 5 \cdot 10^7 \text{ GeV}, \quad (3.26)$$

which makes the results computed in Table 1 viable.

3.5 The case of the exponential tail

Most popular quintessence models assumes an exponential tail in the form:

$$V(\phi) = M^4 e^{-\lambda\phi}. \quad (3.27)$$

By choosing a Jordan frame potential as in eq. (3.27) we get the Einstein frame potential

$$U(\phi) = \frac{M^4 e^{-\lambda\phi}}{8\alpha M^4 e^{-\lambda\phi} + 1}, \quad (3.28)$$

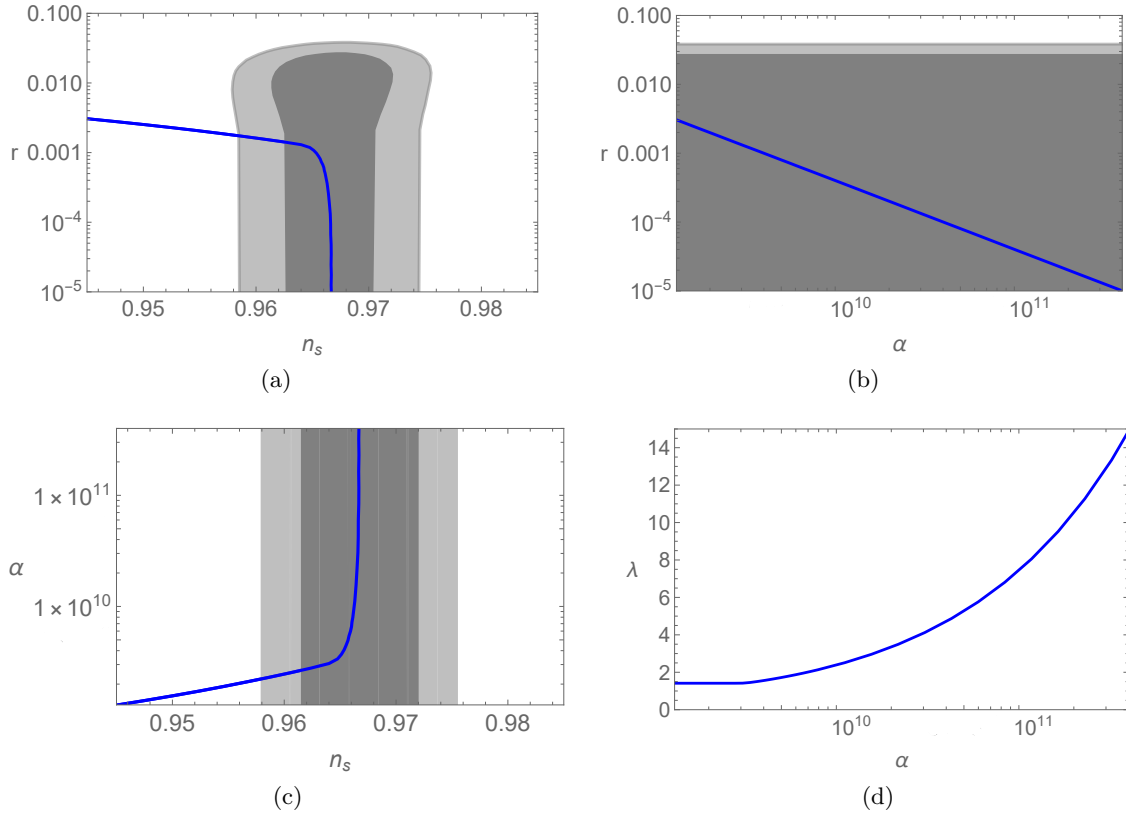


Figure 3: r vs. n_s (a), r vs. α (b), α vs. n_s (c), λ vs. α (d) for the quadratic model with $V(\phi) = V_0 e^{-\lambda\phi}$ for $N_e = 60$. The relation between α and λ is imposed by fixing $A_s \sim 2.1 \cdot 10^{-9}$. The gray regions indicate the 95% (dark-gray) and 68% (light-gray) confidence levels (CL), respectively, based on the latest combination of Planck, BICEP/Keck, and BAO data [37].

and the corresponding the slow-roll parameters

$$\epsilon(\phi) = \frac{\lambda^2}{2} \left(\frac{1}{1 + 8\alpha M^4 e^{-\lambda\phi}} \right)^2, \quad (3.29)$$

$$\eta(\phi) = \frac{\lambda^2 e^{\lambda\phi} (1 - 8M^4 \alpha e^{-\lambda\phi})}{(8M^4 \alpha e^{-\lambda\phi} + 1)^2}. \quad (3.30)$$

From eq. (3.29) we see that:

$$\epsilon(\phi) \sim 0, \quad \text{for } \phi \rightarrow -\infty \quad (3.31)$$

$$\epsilon(\phi) \sim \frac{\lambda^2}{2} \quad \text{for } \phi \rightarrow \infty, \quad (3.32)$$

which implies that to end slow-roll during inflation and have a graceful exit we need $\lambda > \sqrt{2}$. While inflation works very well for this choice of parameters, as shown in Fig. 3, it does not provide a good tail for quintessence. The reason can be seen from Fig. 4. The plot shows the change in the potential by varying the parameter M . The net result of changing M amounts to a translation along the ϕ -axis, while $\phi_{end} - \phi_N$ remains constant (after fixing

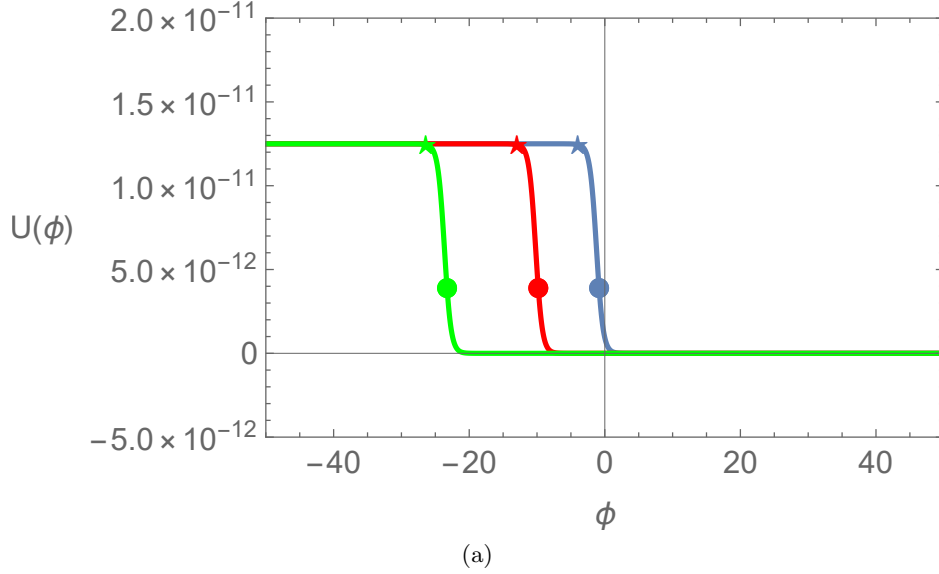


Figure 4: Exponential potential for $M = 10^{-3}$ (blue), $M = 10^{-5}$ (red), $M = 10^{-8}$ (green) and $\alpha = 10^{10}$ and corresponding $\lambda = 2.05$ fixed by setting $A_s \sim 2.1 \cdot 10^{-9}$. We also show ϕ_N (star) and ϕ_{end} (dot) in the same color code. Changing M amounts to a shift in the potential along ϕ -axis.

the other parameters α, λ, N_e), yielding the same results for the inflationary observables. The immediate consequence is that M cannot be used as a parameter to fix, in order to match the observed cosmological constant.

To see this explicitly, consider the tail of eq. (3.28). For $\phi \rightarrow +\infty$, we have:

$$U(\phi) \sim M^4 e^{-\lambda\phi}. \quad (3.33)$$

Once again we want to understand if we can solve the coincidence problem:

$$U(\phi_F) = M^4 e^{-\lambda\phi_F} = \rho_0 \sim 7 \cdot 10^{-121}, \quad (3.34)$$

where ϕ_F is still given by eq. (3.22). For the sake of simplicity, we now consider the case that maximizes eq. (3.22), i.e. gravitational reheating. It can be computed that:

$$\phi_F \sim \phi_{end} + 40, \quad (3.35)$$

where ϕ_{end} is obtained by solving $\epsilon(\phi) = 1$. Hence, we get:

$$U(\phi_F) = \frac{\sqrt{2\lambda} - 2}{16\alpha} e^{-\lambda 40}. \quad (3.36)$$

This implies that the only parameter in the model is λ and the two scales (inflation and dark-energy) cannot be decoupled. Even in the maximal case we cannot solve the coincidence problem unless $\lambda \sim 6.3$ which is too large and cannot reproduce dark-energy behavior. It is then impossible to use this model to achieve a viable quintessential inflation scenario.

4 Quintessential inflation for $F(R_X)_{>2}$

In the following we discuss the case of quintessential inflation for $F(R_X)_{>2}$. For this class of functions, the behavior of $G(\zeta)$ changes drastically and one can see that the equation $G(\zeta) = 0$ always admits a solution for some $\zeta_0 > 0$ (see (2.5)). For any $\zeta > \zeta_0$, the $G(\zeta)$ function is negative. As shown in [33], this configuration works particularly well when considering negative and unbounded from below Jordan frame potentials $V(\phi)$. In fact, such a choice generates an Einstein frame potential U which is positive definite and has an asymptotically flat plateau that allows to perform inflation for $\zeta \rightarrow \zeta_0$ (i.e. $V(\phi) \rightarrow 0$). At the same time for $\zeta \rightarrow +\infty$, the potential U exhibits a tail that asymptotically approaches zero, giving the opportunity to mimic the quintessence behavior without the necessity of introducing a decaying tail behavior to begin with.

In order to give a concrete example, we now focus on the case:

$$F(\zeta) = \zeta + \alpha\zeta^2 \ln(\beta\zeta), \quad (4.1)$$

with $\beta > \alpha/e$, in order to ensure that $F' > 0$ for any $\zeta > \zeta_0$. This specific example allows for an exact solution for eq. (2.5), which reads:

$$\zeta - \alpha\zeta^2 = V(\phi). \quad (4.2)$$

The above equation admits two solutions:

$$\zeta_{\pm} = \frac{1 \pm \sqrt{1 - 4\alpha V(\phi)}}{2\alpha} = \frac{1 \pm \sqrt{1 + 4\alpha|V(\phi)|}}{2\alpha}, \quad (4.3)$$

but the consistency constraints $\zeta \geq \zeta_0 = 1/\alpha$ and $V(\phi) < 0$, suggest

$$\zeta = \zeta_+ = \frac{1 + \sqrt{1 + 4\alpha|V(\phi)|}}{2\alpha}, \quad (4.4)$$

is the only available solution. Using such a solution, we can provide the exact expression of the Einstein frame scalar potential:

$$U(\phi) = \frac{|V(\phi)|}{2 \left(4\alpha|V(\phi)| \ln \left(\frac{\beta(1 + \sqrt{1 + 4\alpha|V(\phi)|})}{2\alpha} \right) + 2\alpha|V(\phi)| + \sqrt{4\alpha|V(\phi)| + 1} - 1 \right)}. \quad (4.5)$$

For $V(\phi) \rightarrow 0$, the above behaves as

$$U(\phi) \approx \frac{1}{8\alpha \left(\ln \left(\frac{\beta}{\alpha} \right) + 1 \right)} \left[1 + \frac{\alpha V(\phi)}{2 \left(\ln \left(\frac{\beta}{\alpha} \right) + 1 \right)} \right], \quad (4.6)$$

while for $V(\phi) \rightarrow -\infty$, as

$$U(\phi) \approx \frac{1}{8\alpha \ln \left(\beta \sqrt{\frac{|V(\phi)|}{\alpha}} \right)} = \frac{1}{8\alpha \left(\frac{1}{2} \ln (|V(\phi)|) + \ln \left(\frac{\beta}{\sqrt{\alpha}} \right) \right)}, \quad (4.7)$$

α	r	n_s	μ/M
10^8	0.03	0.963	0.06
10^{10}	$4 \cdot 10^{-4}$	0.971	$1.6 \cdot 10^{-3}$
10^{12}	$4 \cdot 10^{-6}$	0.972	$2.5 \cdot 10^{-5}$
10^{14}	$4 \cdot 10^{-8}$	0.972	$2.5 \cdot 10^{-7}$
10^{16}	$4 \cdot 10^{-10}$	0.972	$2.5 \cdot 10^{-9}$

Table 2: Results for inflation for the e PV potential in eq. (4.10) with $k = q = 4$ at $N_e = 60$. Predictions for inflation lay inside the 2σ region for r, n_s . The ratio μ/M is fixed by requiring $A_s = 2.1 \cdot 10^{-9}$.

where we emphasize once again that $V(\phi) < 0$. We conclude this preliminary discussion by noting that, if we plug-in an exponential potential with the an asymptotic behaviour

$$V(\phi) \approx -e^{f(\phi)}, \quad (4.8)$$

into eq. (4.7), then the tail of the potential behaves as

$$U(\phi) \approx \frac{1}{f(\phi)}. \quad (4.9)$$

We will use this last result as a guide to construct a working model of quintessential inflation, as we will see in the following subsection.

4.1 Exponential PV potential

Given the result of eq. (4.9), we choose an exponential version¹ of the Peebles-Vilenkin (e PV) potential used in section 3

$$V(\phi) = 1 - e^{V_{PV}(\phi)}, \quad (4.10)$$

with

$$V_{PV}(\phi) = \begin{cases} \frac{\mu^k}{M^q(\phi^k + M^k)} & \phi \leq 0, \\ \frac{\phi^k + \mu^k}{M^{k+q}} & \phi > 0. \end{cases} \quad (4.11)$$

It is possible to show numerically that the parameter β appearing in eq. (4.5) has a negligible effect on the computation of the CMB observables. Moreover, one can see from eq. (4.7) that for realistic choices of α, β the dominant term in the denominator will be given by the $\ln(|V|)$ contribution. Thus, in what follows, we can safely set $\beta = \alpha$ without loss of generality. With this setup it is possible to produce viable predictions for the CMB observables by fixing the two mass scales M, μ without requiring extreme fine tuning to solve the coincidence problem. However, as we can see from Table 2, this setup is physical only for very large α . For this reason, we only compute the slow-roll parameters in the $\alpha \rightarrow \infty$ regime:

$$\epsilon(\phi_N) \sim \frac{1}{8} \alpha^2 k^2 \mu^{2k} \phi^{-2(k+1)} M^{-2q}, \quad (4.12)$$

$$\eta(\phi_N) \sim -\frac{1}{2} \alpha k(k+1) \mu^k \phi^{-k-2} M^{-q}, \quad (4.13)$$

¹We added 1 to the definition of the potential in eq. (4.8) in order to ensure that $V(\phi) \rightarrow 0$ for $\phi \rightarrow -\infty$.

α	$M_{min}[GeV]$	ϕ_F^{min}	$T_{reh}^{max}[GeV]$	$T_{reh}^*[GeV]$
10^8	$5.5 \cdot 10^4$	4.01	$1.2 \cdot 10^6$	$2.9 \cdot 10^7$
10^{10}	$9.8 \cdot 10^4$	4.01	$1.4 \cdot 10^4$	$1.7 \cdot 10^6$
10^{12}	$1.7 \cdot 10^5$	4.01	$1.5 \cdot 10^2$	$1.1 \cdot 10^5$
10^{14}	$3.1 \cdot 10^5$	4.01	1.57	$5.4 \cdot 10^3$
10^{16}	$5.5 \cdot 10^5$	4.01	0.015	305

Table 3: Results for reheating for the e PV potential in eq. (4.10) with $k = q = 4$. The estimated maximum reheating temperature for the model T_{reh}^{max} is below the lower bound T_{reh}^* for every choice of α , this implies that in general the model cannot account for the BBN constraints on overproduction of GWs (see appendix A). However compatibility with observations are restored if one assumes production of heavy particles in the early universe.

and the number of e-folds can be integrated explicitly giving:

$$N_e \sim \frac{2\mu^{-k}\phi^{k+2}M^q}{\alpha k(k+2)}. \quad (4.14)$$

Finally, the CMB observables read:

$$r \sim \frac{1}{12\pi^2\alpha A_s}, \quad (4.15)$$

$$n_s \sim 1 - \frac{k+1}{k+2} \frac{2}{N_e}, \quad (4.16)$$

$$A_s \sim \frac{2^{-\frac{5k+8}{k+2}}\mu^{-2k}M^{2q}(\alpha k(k+2)N_e\mu^k M^{-q})^{\frac{2(k+1)}{k+2}}}{3\pi^2\alpha^3 k^2}. \quad (4.17)$$

We note that the limits for r and n_s are the same as the ones shown in eqs. (3.7) and (3.8). Indeed, it can be easily proven that the current setup and the one in section 3.1 are actually equivalent in the inflationary region for $\alpha \rightarrow \infty$. After inflation is over, kination and reheating follow (see sections 3.2 - 3.3). The reheating temperature must satisfy the bound $T_{reh} > T_{BBN} \sim 10^{-2}$ GeV. After reheating takes place, radiation eventually starts dominating. During the expansion, the scalar field ϕ_F freezes at the value given by eq. (3.22).

In order to have a working quintessential inflation mechanism, we need to satisfy two more requirements. The first one is that the value of the scalar field potential energy-density at freezing must match the value of the observed energy density of dark energy today (coincidence requirement). By using eqs. (4.7) and (4.10), we find:

$$U(\phi_F) \approx \frac{M^k}{4\alpha(\phi_F^k + \mu^k)} = \rho_0 \sim 7 \cdot 10^{-121}. \quad (4.18)$$

Second, we need to check that the barotropic parameter at the present day w_0 for the quintessential tail is within the Planck observational bounds [39]. In order for this to happen we need to make sure that the scalar field unfreezes only at the time of matter-dark energy equality. In other words, the field stays frozen until recent times and only unfreezes when it becomes dominating. The field then thaws and starts slow-rolling down its potential. This happens provided that the frozen scalar field does not hit the tracker before it starts dominating (see section 3.4). The equation for the barotropic parameter in w_ϕ is given by

eq. (3.25). Once again the field will not substantially evolve till the present day, with $\phi_0 \simeq \phi_F$ and $w_\phi \approx -1$.

We show in Table 3 the results for the case $k = q = 4$. We only report the values of α for which we obtain viable CMB observables. The value M_{\min} is the minimum value of the mass scale for the potential in eq. (4.10) necessary to avoid the tracker solution and let the field unfreeze only at matter-dark energy equality. The corresponding ϕ_F^{\min} is obtained by imposing the solution of the coincidence problem in eq. (4.18). The reheating temperature is computed by means of eq. (3.19) by setting $M = M_{\min}$ and $\phi = \phi_{\min}$. Finally, we need to check if the model can satisfy the constraints on T_{reh} coming from GW overproduction. During kination, the $w = 1$ stiff period induces a spike in the density of the GWs, potentially spoiling BBN. This can be avoided if T_{reh} is large enough. The details on the calculation can be found in appendix A, while we show in Table 3 an estimate of the lower bound T_{reh}^* (depending on the value of α) that avoids GW overproduction.

Unfortunately, we always have $T_{reh}^{max} < T_{reh}^*$ hence the model is not in general viable. As before, compatibility with observation can be restored if we assume the gravitational production of very massive particles after the inflationary era [14] which naively relaxes the reheating temperature bound to the one showed in eq. (3.26), making the results computed in Table 3 viable again.

4.2 A note on the exponential tail

Given eq. (4.7), one can try to reproduce an exponential tail by choosing a Jordan frame potential in the form of a double exponential:

$$V(\phi) = 1 - e^{\sigma e^{\lambda\phi}}. \quad (4.19)$$

The Einstein frame tail would then behave as:

$$U(\phi) \approx \frac{e^{-\lambda\phi}}{4\alpha\lambda}. \quad (4.20)$$

However, this setup cannot be used to generate a quintessential tail.

Consider the slow-roll parameter $\epsilon(\phi) = \frac{U'(\phi)^2}{2U(\phi)^2}$ with $U(\phi)$ given by eq. (4.5). It can be straightforwardly computed that this function is a monotonically increasing function with the following limits:

$$\epsilon(\phi) \sim 0, \quad \text{for } \phi \rightarrow -\infty, \quad (4.21)$$

$$\epsilon(\phi) \sim \frac{\lambda^2}{2}, \quad \text{for } \phi \rightarrow \infty, \quad (4.22)$$

which implies that to end slow-roll during inflation and have a graceful exit we need $\lambda > \sqrt{2}$. Once again the same parameter determines the behavior at inflation and in the tail, this implies that the two scales cannot be decoupled. Since this setup is equivalent to the one presented in 3.5 we conclude that it is not viable.

5 Conclusions

We have studied modeling quintessential inflation in the context of $F(R, X)$ Palatini gravity. In particular, we considered a potential in the form of the generalized Peebles-Vilenkin (PV)

potential for a quadratic $F(R, X)$. We proved that the model generates viable quintessential inflation in the case $k = q = 4$ with a mass scale $M \sim 10^3 - 10^5$ GeV, providing the right inflationary observables, a solution for the coincidence problem and a prediction for the barotropic parameter $w_\phi \approx -1$. The model predicts in general a value of $T_{reh} < 10^5$ GeV, which contradicts the lower bound on T_{reh} necessary to avoid overproduction of GWs during kination. However, compatibility with observations can be restored if we assume production of heavy particles $\sim 10^{-6}m_P$, which later-on decay in the SM sector. This relaxes the bound to $1 \text{ MeV} \leq T_{reh} \leq 5 \cdot 10^7$ GeV, which is compatible with our predictions.

We also considered an example for a model $F(R, X)_{>2}$, in the form $F(R_X) = R_X + \alpha R_X^2 \ln(\alpha R_X)$ with a Jordan frame potential given by an exponential version of the PV potential, characterized by two mass scales μ, M . The model predicts viable quintessential inflation for $k = q = 4$ with a mass scale of order $M \sim 10^5$ GeV which solves the coincidence problem and $1 \text{ MeV} < \mu < 10^3$ GeV fixed by the amplitude of scalar perturbations A_s . As in the previous case the model predicts in general a value of $T_{reh} < 10^5$ GeV which cannot be accepted if one considers the lower bound on T_{reh} necessary to avoid overproduction of GWs during kination. The solution is again to assume production of heavy particles in the early Universe.

We also showed that a quintessential tail given by a simple exponential, although generating very good inflationary results, does not provide a solution for the coincidence problem (in both the $F(R, X)$ models).

All in all, this study demonstrated that $F(R, X)$ Palatini gravity is a promising framework for constructing viable quintessential inflation models, although it can be challenging to address successfully all the relevant constraints and, in particular, the overproduction of primordial gravitational waves during kination.

Acknowledgments

KD is supported (in part) by the STFC consolidated Grant: ST/X000621/1. This work was supported by the Estonian Research Council grants PRG1055, RVTT3, RVTT7 and the CoE program TK202 “Foundations of the Universe”. This article is based upon work from COST Actions COSMIC WISPerS CA21106 and CosmoVerse CA21136, supported by COST (European Cooperation in Science and Technology).

A Constraints from the overproduction of GWs

In the following we briefly compute an estimate on the reheating temperature necessary to avoid overproduction of GWs during kination (see for example [40] for the details).

In order to respect the bounds from BBN we need to constraint the intensity:

$$\Omega_{peak} h^2 = \int_{\nu_{BBN}}^{\nu_{end}} \frac{\Omega_{GW} h^2}{\nu} d\nu \leq \frac{7}{8} \left(\frac{4}{11} \right)^{4/3} \Omega h^2 \Delta N_{\text{eff}}, \quad (\text{A.1})$$

where Ω_{GW} is the spectrum of the gravitational waves, $\Omega_r h^2 \sim 2.47 \cdot 10^{-5}$ is the relic density of radiation, $\nu_{BBN} \sim 10^{-11} \text{ Hz}$ and $\Delta N_{\text{eff}} \sim 0.17$ the extra relativistic degrees of freedom during BBN given by the current Planck bound [39].

The above can be related to the reheating temperature as follows. Consider the frequencies ν_{end}, ν_{reh} corresponding to the GW modes that reenter the horizon respectively at

the end of inflation and at reheating. We have:

$$\nu_{end} = \frac{H_{end}}{2\pi} \frac{a_{end}}{a_0}, \quad (\text{A.2})$$

$$\nu_{reh} = \nu_{end} \left(\frac{H_{end}}{H_{reh}} \right)^{2/3}, \quad (\text{A.3})$$

with

$$H_{reh} = \pi \sqrt{\frac{g_{reh}^*}{90}} T_{reh}^2. \quad (\text{A.4})$$

Finally, between the end of the inflation and reheating we have that

$$\Omega_{peak} = \Omega_{GW}^{rd} \frac{\nu_{end}}{\nu_{reh}}, \quad (\text{A.5})$$

where $\Omega_{GW}^{rd} \propto H_{end}^2$, is the GW density parameter of the modes that reenter the horizon during radiation domination. By comparing (A.1) with (A.5) and using (A.2)-(A.4) we get a lower bound on T_{reh} .

References

- [1] E. J. Copeland, M. Sami and S. Tsujikawa, *Dynamics of dark energy*, *Int. J. Mod. Phys. D* **15** (2006) 1753 [[hep-th/0603057](#)].
- [2] S. Tsujikawa, *Quintessence: A Review*, *Class. Quant. Grav.* **30** (2013) 214003 [[1304.1961](#)].
- [3] A. A. Starobinsky, *A New Type of Isotropic Cosmological Models Without Singularity*, *Phys. Lett.* **B91** (1980) 99.
- [4] A. H. Guth, *The Inflationary Universe: A Possible Solution to the Horizon and Flatness Problems*, *Phys.Rev.* **D23** (1981) 347.
- [5] A. D. Linde, *A New Inflationary Universe Scenario: A Possible Solution of the Horizon, Flatness, Homogeneity, Isotropy and Primordial Monopole Problems*, *Phys.Lett.* **B108** (1982) 389.
- [6] A. Albrecht and P. J. Steinhardt, *Cosmology for Grand Unified Theories with Radiatively Induced Symmetry Breaking*, *Phys.Rev.Lett.* **48** (1982) 1220.
- [7] P. J. E. Peebles and A. Vilenkin, *Quintessential inflation*, *Phys. Rev. D* **59** (1999) 063505 [[astro-ph/9810509](#)].
- [8] G. Felder, L. Kofman and A. Linde, *Instant preheating*, *Physical Review D* **59** (1999) .
- [9] A. H. Campos, H. C. Reis and R. Rosenfeld, *Preheating in quintessential inflation*, *Phys. Lett. B* **575** (2003) 151 [[hep-ph/0210152](#)].
- [10] B. Feng and M. Li, *Curvaton reheating in non-oscillatory inflationary models*, *Physics Letters B* **564** (2003) 169–174.
- [11] J. C. Bueno Sanchez and K. Dimopoulos, *Curvaton reheating allows TeV Hubble scale in NO inflation*, *JCAP* **11** (2007) 007 [[0707.3967](#)].
- [12] L. H. Ford, *Gravitational particle creation and inflation*, *Phys. Rev. D* **35** (1987) 2955.
- [13] E. J. Chun, S. Scopel and I. Zaballa, *Gravitational reheating in quintessential inflation*, *JCAP* **07** (2009) 022 [[0904.0675](#)].
- [14] J. de Haro, *Reheating formulas in quintessential inflation via gravitational particle production*, *Phys. Rev. D* **109** (2024) 023517 [[2310.02245](#)].

- [15] K. Dimopoulos and T. Markkanen, *Non-minimal gravitational reheating during kination*, *JCAP* **06** (2018) 021 [1803.07399].
- [16] T. Opferkuch, P. Schwaller and B. A. Stefanek, *Ricci Reheating*, *JCAP* **07** (2019) 016 [1905.06823].
- [17] D. Bettoni, A. Lopez-Eiguren and J. Rubio, *Hubble-induced phase transitions on the lattice with applications to Ricci reheating*, *JCAP* **01** (2022) 002 [2107.09671].
- [18] I. Dalianis and G. P. Kodaxis, *Reheating in Runaway Inflation Models via the Evaporation of Mini Primordial Black Holes*, *Galaxies* **10** (2022) 31 [2112.15576].
- [19] M. Riajul Haque, E. Kpatcha, D. Maity and Y. Mambrini, *Primordial black hole reheating*, *Phys. Rev. D* **108** (2023) 063523 [2305.10518].
- [20] K. Dimopoulos and L. Donaldson-Wood, *Warm quintessential inflation*, *Phys. Lett. B* **796** (2019) 26 [1906.09648].
- [21] J. a. G. Rosa and L. B. Ventura, *Warm Little Inflaton becomes Dark Energy*, *Phys. Lett. B* **798** (2019) 134984 [1906.11835].
- [22] K. Dimopoulos and C. Owen, *Quintessential Inflation with α -attractors*, *JCAP* **06** (2017) 027 [1703.00305].
- [23] J. de Haro and L. A. Saló, *A Review of Quintessential Inflation*, *Galaxies* **9** (2021) 73 [2108.11144].
- [24] D. Bettoni and J. Rubio, *Quintessential Inflation: A Tale of Emergent and Broken Symmetries*, *Galaxies* **10** (2022) 22 [2112.11948].
- [25] N. Jaman and M. Sami, *What Is Needed of a Scalar Field If It Is to Unify Inflation and Late Time Acceleration?*, *Galaxies* **10** (2022) 51 [2202.06194].
- [26] K. Dimopoulos and S. Sánchez López, *Quintessential inflation in Palatini $f(R)$ gravity*, *Phys. Rev. D* **103** (2021) 043533 [2012.06831].
- [27] K. Dimopoulos, A. Karam, S. Sánchez López and E. Tomberg, *Modelling Quintessential Inflation in Palatini-Modified Gravity*, *Galaxies* **10** (2022) 57 [2203.05424].
- [28] K. Dimopoulos, A. Karam, S. Sánchez López and E. Tomberg, *Palatini R^2 quintessential inflation*, *JCAP* **10** (2022) 076 [2206.14117].
- [29] I. D. Gialamas, A. Karam, T. D. Pappas and E. Tomberg, *Implications of Palatini gravity for inflation and beyond*, *Int. J. Geom. Meth. Mod. Phys.* **20** (2023) 2330007 [2303.14148].
- [30] J. J. Terente Díaz, K. Dimopoulos, M. Karčiauskas and A. Racioppi, *Quintessence in the Weyl-Gauss-Bonnet model*, *JCAP* **02** (2024) 040 [2310.08128].
- [31] T. Koivisto and H. Kurki-Suonio, *Cosmological perturbations in the palatini formulation of modified gravity*, *Class. Quant. Grav.* **23** (2006) 2355 [astro-ph/0509422].
- [32] F. Bauer and D. A. Demir, *Inflation with Non-Minimal Coupling: Metric versus Palatini Formulations*, *Phys. Lett.* **B665** (2008) 222 [0803.2664].
- [33] C. Dioguardi and A. Racioppi, *Palatini $F(R, X)$: A new framework for inflationary attractors*, *Phys. Dark Univ.* **45** (2024) 101509 [2307.02963].
- [34] C. Dioguardi, A. Racioppi and E. Tomberg, *Beyond (and back to) palatini quadratic gravity and inflation*, *Journal of Cosmology and Astroparticle Physics* **2024** (2024) 041.
- [35] N. Bostan, R. H. Dejarah, C. Dioguardi and A. Racioppi, *Natural inflation in Palatini $F(R, X)$* , **2503.16324**.
- [36] C. Dioguardi, A. Racioppi and E. Tomberg, *Slow-roll inflation in Palatini $F(R)$ gravity*, *JHEP* **06** (2022) 106 [2112.12149].

- [37] BICEP, KECK collaboration, *Improved Constraints on Primordial Gravitational Waves using Planck, WMAP, and BICEP/Keck Observations through the 2018 Observing Season*, *Phys. Rev. Lett.* **127** (2021) 151301 [[2110.00483](#)].
- [38] PLANCK collaboration, *Planck 2018 results. X. Constraints on inflation*, *Astron. Astrophys.* **641** (2020) A10 [[1807.06211](#)].
- [39] Planck Collaboration and A. et al., *Planck 2018 results - vi. cosmological parameters*, *A&A* **641** (2020) A6.
- [40] C. Chen, S. Jyoti Das, K. Dimopoulos and A. Ghoshal, *Flipped Rotating Axion Non-minimally Coupled to Gravity: Baryogenesis and Dark Matter*, [2502.08720](#).